



Long tails in deep columns of natural and anthropogenic tropospheric tracers

J. David Neelin,^{1,2} Benjamin R. Lintner,^{1,2,3} Baijun Tian,⁴ Qinbin Li,^{1,4} Li Zhang,¹ Prabir K. Patra,⁵ Moustafa T. Chahine,⁴ and Samuel N. Stechmann^{1,6}

Received 16 November 2009; revised 20 January 2010; accepted 27 January 2010; published 4 March 2010.

[1] Simple prototypes for forced advection-diffusion problems are known to produce passive tracer distributions that exhibit approximately exponential or stretched exponential tails. Having previously found an approximately exponential tail for the column integrated water vapor (CWV) distribution under high precipitation conditions, we conjectured that if such prototypes are relevant to more complex tropospheric tracer problems, we should find such tails for a wide set of tracers. Here it is shown that such tails are indeed ubiquitous in observed, model, and reanalysis data sets for a variety of tracers, either column integrated or averaged through a deep layer, including CO and CO₂. The long tails in CWV are associated with vertical transport and can occur independent of a local precipitation sink. These non-Gaussian distributions can have consequences for source attribution studies of anthropogenic tracers, and for mechanisms of precipitation extremes; the properties of the tails may help constrain model tracer simulations.

Citation: Neelin, J. D., B. R. Lintner, B. Tian, Q. Li, L. Zhang, P. K. Patra, M. T. Chahine, and S. N. Stechmann (2010), Long tails in deep columns of natural and anthropogenic tropospheric tracers, *Geophys. Res. Lett.*, 37, L05804, doi:10.1029/2009GL041726.

1. Introduction

[2] Variations in tracer concentrations through deep layers of the troposphere represent an important feature of the transport process and can be retrieved by satellite nadir-viewing instruments for water vapor and certain other tracers [Hilburn and Wentz, 2008; Drummond and Mand, 1996; Chahine et al., 2008]. A probability distribution for column integrated water vapor (CWV) with a long tail, i.e., much longer than Gaussian, was recently encountered [Neelin et al., 2009] in microwave retrievals, associated with high precipitation conditions at short time scales. Simple passive tracer advection-diffusion problems with a forcing that maintains a gradient can produce distributions with

Gaussian core and approximately exponential tails [Shraiman and Siggia, 1994; Pierrehumbert, 2000; Ngan and Pierrehumbert, 2000; Bourlioux and Majda, 2002] and distributions with exponential tails have been simulated for stratospheric tracers [Hu and Pierrehumbert, 2001, 2002]. To the extent that these elegant prototypes are relevant to more complex tropospheric tracers with surface sources and a variety of sinks, one can anticipate such tails for both natural and anthropogenic tropospheric column tracer values. Analysis of multiple tracers can potentially elucidate mechanisms for extreme events in both precipitation and column loadings of important chemical species. We thus examine observed, model, and reanalysis data sets for deep-column integrated tracers, including CWV, carbon monoxide (CO) and new retrievals of carbon dioxide (CO₂). These span a considerable range of tracer lifetimes and source conditions, and the latter two represent important tracers with anthropogenic sources. Simulated distributions for nitrous oxide, ozone and an idealized tracer are included in the auxiliary material to strengthen the argument that long tails are widespread.¹

[3] It is far from obvious that long tails should survive vertical averaging. Long tails have been noted in distributions of vertical differences in potential temperature [Schertzer and Lovejoy, 1985], point differences in stratospheric N₂O concentrations [Sparling and Bacmeister, 2001], and in tropopause temperature [Richard et al., 2006] but if fluctuations were decorrelated in the vertical, one might expect the central limit theorem to apply to vertical averages. We first outline an argument for why tracer forcing that maintains a vertical gradient might produce long tails in column integrated values in the presence of conditions on vertical and horizontal motions that are widely met in the troposphere. To see how this plays out quantitatively for complex three-dimensional, inhomogeneous flow fields, a variety of source-sink characteristics and, in the case of water vapor, an active rather than passive tracer, motivates the observational and model analysis forming the heart of this paper.

[4] The equation for a tracer concentration q (by mass) is,

$$\partial_t q + \mathbf{v} \cdot \nabla q + w \partial_z q - \kappa \nabla^2 q - \partial_z \kappa_v \partial_z q = -S \quad (1)$$

with \mathbf{v} , w horizontal and vertical velocity components, κ , κ_v horizontal and vertical diffusivities, and S representing any internal sink (or source) within the atmosphere (e.g., conversion to another chemical species or precipitation). For a wide class of atmospheric tracer problems the primary source is via a surface flux F . For some anthropogenic tracers there is essentially no internal sink, but when studying

¹Department of Atmospheric and Oceanic Sciences, University of California, Los Angeles, California, USA.

²Institute of Geophysics and Planetary Physics, University of California, Los Angeles, California, USA.

³Department of Environmental Sciences, Rutgers- State University of New Jersey, New Brunswick, New Jersey, USA.

⁴Jet Propulsion Laboratory, California Institute of Technology, Pasadena, California, USA.

⁵Frontier Research Center for Global Change, Yokohama, Japan.

⁶Department of Mathematics, University of California, Los Angeles, California, USA.

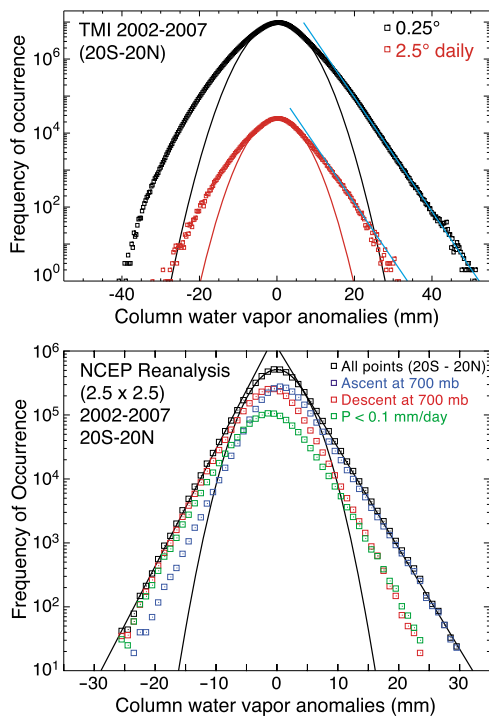


Figure 1. Distribution (as frequency of occurrence) of column water vapor anomalies at each spatial point (top) from TMI observations over the tropics (20S–20N) at two resolutions: 0.25 degrees, instantaneous in time and 2.5 degrees, daily average; (bottom) for NCEP reanalysis daily average (20N–20S), showing the distribution for all values, the distribution separated according to ascending/descending vertical motion in the midtroposphere, and the distribution conditioned on a low-rainfall criterion. The parabolas (light curves) show a Gaussian fit to the core of each distribution, while the straight lines provide a reference for the approximately exponential tails.

anomalies of tracer concentrations, the long-term increasing trend is removed, and this is mathematically equivalent to a sink (see auxiliary material). In either case, a vertical gradient is maintained by surface flux input into the atmospheric boundary layer (ABL), relative to the free atmosphere. Once vertical advection lofts the tracer, horizontal advection acts on resulting horizontal gradients.

[5] An idealized set-up of equation 1 by *Bourlioux and Majda* [2002] motivates our hypothesis that we should commonly anticipate long tails for anomalies through the depth of the troposphere and provides a simplest-case conjectured physical explanation. Their case of winds and gradient constant in one direction, say, vertical, yields tracer anomalies constant in this direction. The deep structures of horizontal and vertical velocity anomalies commonly encountered through the depth of the troposphere will likewise tend to yield coherent vertical structures of tracer variations, and large variations of vertically integrated tracer (see auxiliary material for more detailed considerations and review of prototypes). We thus anticipate that the results from theoretical prototypes can provide qualitative guidance for analyzing distributions of column tracers, modified for expected asymmetry between upward and downward motion. The close analogy between

the problems suggests that long tails should be ubiquitous in column concentrations, for which we provide initial evidence here.

2. Column Water Vapor

[6] We begin by examining observations of CWV, due to its long record of validated satellite observations, its importance for meteorological problems, and because it is standardly included in many model systems. Figure 1 (top) shows the distribution of CWV anomalies from the Tropical Rainfall Measuring Mission (TRMM) Microwave Imager (TMI) [*Hilburn and Wentz*, 2008] from 2002–2007. Examining anomalies (with respect to a 30 day average) is analogous to the procedure used in prototype systems; this avoids complexities associated with the climatological spatial distribution of humidity or relative humidity [*Zhang et al.*, 2003; *Ryoo et al.*, 2009] to focus on short-term, transport-induced variations. The distribution is shown as counts per bin since this is useful when doing subsets of the total (normalizing simply shifts the figure).

[7] At high resolution ($0.25^\circ \times 0.25^\circ$) and effectively instantaneous in time (the instrument scan), the tails are considerably broader than a Gaussian fit to the core of the distribution. The range is on the order of the mean water vapor (typically 40–55 mm). There is a marked asymmetry between negative and positive tails of the distribution, with the positive side having a long exponential range. On the negative side, the tail tapers off more quickly, but attempting to fit it with a Gaussian would considerably overestimate the core. If the long tails are associated with vertical advection, as will be elaborated below, there are two clear sources of asymmetry between upward and downward processes (see examples in auxiliary material). First, upward motion is stronger in convecting regions compared to compensating descent over broader surrounding regions; and second, the effects of downward advection are limited by drying out the column above the ABL, a known association with occurrences of low column water vapor [*Holloway and Neelin*, 2009].

[8] Averaging in space and time should reduce this asymmetry and permit comparison to model products in which convection is parameterized. Figure 1 (top) includes TMI averaged to $2.5^\circ \times 2.5^\circ$ in space, with a rough daily average from the two TRMM satellite passes each day. For space-time averages over a large number of independent realizations, the distribution should eventually tend toward Gaussian, but on these scales of practical interest the tails extend substantially beyond the Gaussian core. As expected, the asymmetry is reduced.

[9] Figure 1 (bottom) shows a CWV distribution at $2.5^\circ \times 2.5^\circ$ resolution, for daily averages over 2002–2007 from the National Center for Environmental Prediction (NCEP) reanalysis product [*Kalnay et al.*, 1996]. Again the tails of the distribution fall off less rapidly than the Gaussian core. Moderate asymmetry between positive and negative tails is also apparent. Both tails have a long, approximately exponential range. The reanalysis provides dynamical fields that can confirm the role of vertical advection in producing these tails. To assess this, Figure 1 (bottom) provides distributions divided into values associated with ascending and descending motions. Vertical motion at the 700 mbar level in the lower free troposphere is used since this level is located within the

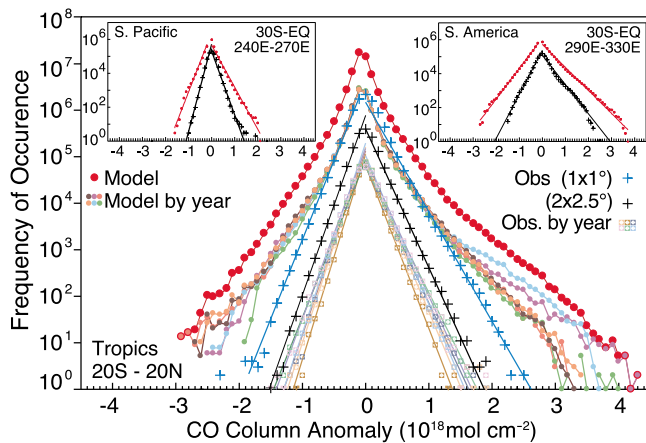


Figure 2. Distribution of column-integrated anomalies of carbon monoxide (10^{18} molecules cm^{-2}) from MOPITT observational estimates for 2001–2006 at $1 \times 1^\circ$ (blue+) and $2 \times 2.5^\circ$ (black+) and for individual years at $2 \times 2.5^\circ$ (pastel squares) and GEOS-Chem atmospheric chemistry model simulations at $2 \times 2.5^\circ$ for 2000–2005 (red dots) and for individual years (pastel dots), for the entire tropics (20S–20N; main panel). Insets show distributions for subregions in a South Pacific region and region that includes South America for MOPITT (red dots) and GEOS-Chem (black+).

layer of strong vertical gradient of specific humidity. The positive tail of the full distribution is clearly associated with ascending points, and conversely for the negative tail. We can further assess whether a local sink associated with precipitation is important to these tails by considering points with small rainfall (less than 0.1 mm/day), for which the local loss of moisture is negligible. The distribution nonetheless has exponential tails similar to the case of descending motions. The positive and negative tails of this small-rainfall distribution are fairly symmetric, consistent with the hypothesis that strong upward vertical velocity associated with latent heat release in regions of precipitation contributes to slower decay of the positive tail. The presence of the positive tail makes clear that the basic process of creating the tail does not require a local loss process.

3. Carbon Monoxide

[10] Carbon monoxide is a tracer with an intermediate lifetime (on the order of two months) [Levy, 1971] for which satellite retrievals are available from the Measurements of Pollution in the Troposphere (MOPITT) mission [Drummond and Mand, 1996; Pan et al., 1998]. Surface sources, such as biomass burning, tend to be heterogeneously distributed. Figure 2 shows distributions of column CO from the MOPITT V3 data set from 2001–2006 at $1^\circ \times 1^\circ$ and $2^\circ \times 2.5^\circ$ resolution, over the tropics and two example sub-regions (a South Eastern Pacific region with relatively low sources and a region spanning South America with fairly strong sources from biomass burning). In each case, the tails are close to exponential over a broad range, with small cores. The slope is modified only slightly by horizontal averaging.

[11] Without the theoretical prototype, a concern might be whether some unknown noise process in the retrievals could

introduce the exponential tails, although regional differences in the slopes of the tails argue against this. Comparison to simulations of CO in the GEOS-Chem atmospheric chemistry model [Bey et al., 2001] in Figure 2 clearly shows that such tails are produced by physical processes. The simulated distributions tend to have a peaked core and broader tails. These are reminiscent of stretched exponential distributions from cases in Bourlioux and Majda [2002], in which the slopes of the tails are determined not only by the imposed gradient and flow variation amplitude, but by assumptions regarding the flow temporal variability (see auxiliary material). Thus it is possible that higher temporal coherence in the vertical transport contributes to wider tails in the model. The MOPITT infrared retrieval may also underestimate the tails, since it is unavailable in cloudy pixels, thus excluding points with high vertical transport by moist convection. The simulated tails vary among regions in a manner consistent with observations. Although asymmetry between high and low tails is smaller than in CWV, the model asymmetry tends to be in the same sense as the observations. The statistics are stable enough that most features of the distribution are reproduced with a single year of data, although for the model, variation among estimates from individual years may be seen in the positive tail. These are associated with interannual variations in the transport (sources are fixed in these simulations). Year-to-year variations are smaller in the observations.

4. Carbon Dioxide

[12] For carbon dioxide (Figure 3), we examine a pre-release daily data set based on new retrievals [Chahine et

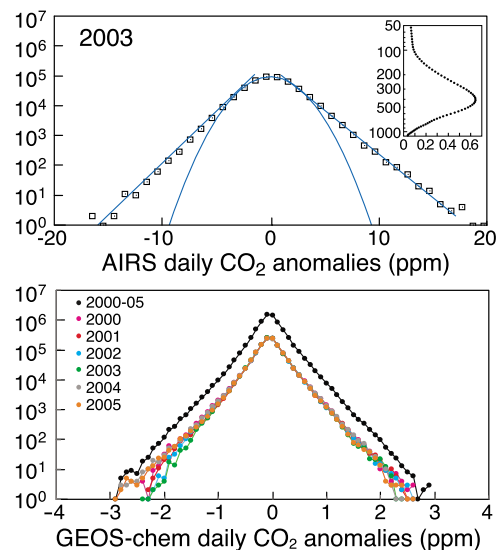


Figure 3. Distribution of anomalies of carbon dioxide for the tropics (20S–20N) (top) from AIRS observational estimates at $2.5^\circ \times 2.5^\circ$ for a deep vertical average that emphasizes the mid-troposphere (weighting function shown in inset) for 2003. A Gaussian core is fit to points above half-maximum. (bottom) From GEOS-Chem simulations vertically averaged with the AIRS weighting function for 2000–2005 (black dots) and for individual years (colored dots).

al., 2005, 2008] from the Atmospheric Infrared Sounder [AIRS; *Chahine et al.*, 2006]. The observations are shown as vertical average concentrations with a deep vertical weighting that is a maximum in the middle and upper troposphere, computed for the available year 2003. Again, long tails with an approximately exponential range give a distribution much wider than Gaussian. To compare to GEOS-Chem simulations [Suntharalingam et al., 2003], the model CO₂ anomalies are convolved with the AIRS weighting function. The GEOS-Chem distribution has a narrower core and a wide exponential range. However, the tails are much steeper, by more than a factor of 5. This is on the same order as differences in monthly mean gradient in the midtroposphere between model and retrieval [Chahine et al., 2008].

5. Discussion

[13] In the case of MOPITT CO, a data set with a long track record of validation [Drummond and Mand, 1996; Pan et al., 1998; Emmons et al., 2009] exhibits the property of interest. In the case of CO₂, the retrieval is still in the process of assessment and comparison to models is a two-way interaction. Thus, that the daily variations exhibit a property consistent with other tracers and model simulations is useful—the form of the long-tailed distribution is not an artifact but rather boosts confidence that the retrieval captures large-scale structures involved in transport. However, the issue of differing magnitudes [Chahine et al., 2008] is reinforced, while the long tails suggest a substantial set of in situ observations will be required for further validation. Furthermore, standard inverse modeling methods for estimating emissions given observed atmospheric concentrations are derived from Bayes' theorem with the assumption of Gaussian errors [Rodgers, 2000]. The wider than Gaussian distribution will have to be taken into account as such data are used for monitoring and attributing emissions of CO₂, CO and very likely other chemical species.

[14] Overall, these results provide strong initial observational evidence for the prediction that long, approximately exponential tails should be widely found in distributions of atmospheric tracers with a wide variety of source/sink properties. Models, even at fairly coarse horizontal resolution typical of atmospheric chemistry models, are capable of capturing this behavior qualitatively, despite large diffusion used to parameterize sub-gridscale eddy transports. This is less surprising when one considers that the observations are made with a finite horizontal footprint and then averaged to the scale of the models, so the effective diffusivity is associated with real turbulent transports across this scale. Quantitatively, characteristics such as the slopes and asymmetry of the tails and the variation of these with meteorological and source conditions of different regions appear sufficiently challenging to simulate that these provide useful metrics for validating models. Unraveling the dominant contributions invites theoretical work with cases that span the gap between the simplest prototypes and the observations. Finally, the presence of these tails in passive chemical tracers, together with the similarity of the CWV tails for both raining and non-raining conditions, suggests that despite the active role of moisture in convective rainfall, the mechanism for producing the long tails in water vapor (and associated strong rainfall

events) strongly inherits properties from the passive transport prototypes.

[15] **Acknowledgments.** This research was supported in part by NSF grant ATM-0645200, NOAA grant NA08OAR4310882, NASA grant NNX09AF07G, and NOAA Climate and Global Change Postdoctoral Fellowship.

References

- Bey, I., et al. (2001), Global modeling of tropospheric chemistry with assimilated meteorology: Model description and evaluation, *J. Geophys. Res.*, *106*, 23,073–23,095.
- Bourlioux, A., and A. J. Majda (2002), Elementary models with probability distribution function intermittency for passive scalars with a mean gradient, *Phys. Fluids*, *14*, 881–897, doi:10.1063/1.1430736.
- Chahine, M. T., et al. (2006), AIRS: Improving weather forecasting and providing new data on greenhouse gases, *Bull. Am. Meteorol. Soc.*, *87*, 911–926.
- Chahine, M. T., C. Barnet, E. T. Olsen, L. Chen, and E. Maddy (2005), On the determination of atmospheric minor gases by the method of vanishing partial derivatives with application to CO₂, *Geophys. Res. Lett.*, *32*, L22803, doi:10.1029/2005GL024165.
- Chahine, M., L. Chen, P. Dimotakis, X. Jiang, Q. B. Li, E. Olsen, T. Pagano, J. Randerson, and Y. Yung (2008), Satellite remote sounding of middle tropospheric CO₂, *Geophys. Res. Lett.*, *35*, L17807, doi:10.1029/2008GL035022.
- Drummond, J. R., and G. S. Mand (1996), The measurements of pollution in the troposphere (MOPITT) instrument: Overall performance and calibration requirements, *J. Atmos. Ocean. Technol.*, *13*, 314–320.
- Emmons, L. K., D. P. Edwards, M. N. Deeter, J. C. Gille, T. Campos, P. Nedelec, P. Novelli, and G. Sachse (2009), Measurements of pollution in the troposphere (MOPITT) validation through 2006, *Atmos. Chem. Phys.*, *9*, 1795–1803.
- Hilburn, K. A., and F. J. Wentz (2008), Intercalibrated passive microwave rain products from the unified microwave ocean retrieval algorithm (UMORA), *J. Appl. Meteor. Clim.*, *47*, 778–794.
- Holloway, C. E., and J. D. Neelin (2009), Moisture vertical structure, column water vapor, and tropical deep convection, *J. Atmos. Sci.*, *66*, 1665–1683.
- Hu, Y., and R. T. Pierrehumbert (2001), The advection-diffusion problem for stratospheric flow. Part I: Concentration probability distribution function, *J. Atmos. Sci.*, *58*, 1493–1510.
- Hu, Y., and R. T. Pierrehumbert (2002), The advection-diffusion problem for stratospheric flow. Part II: Concentration probability distribution function of tracer gradients, *J. Atmos. Sci.*, *59*, 2830–2845.
- Kalnay, E., et al. (1996), The NCEP/NCAR 40-year reanalysis project, *Bull. Am. Meteorol. Soc.*, *77*, 437–471.
- Levy, H. (1971), Normal atmosphere: Large radical and formaldehyde concentrations predicted, *Science*, *173*, 141–143.
- Neelin, J. D., O. Peters, and K. Hales (2009), The transition to strong convection, *J. Atmos. Sci.*, *66*, 2367–2384.
- Ngan, K., and R. T. Pierrehumbert (2000), Spatially correlated and inhomogeneous random advection, *Phys. Fluids*, *12*(4), 822–834, doi:10.1063/1.870338.
- Pan, Y. H., J. C. Gille, D. P. Edwards, P. L. Bailey, and C. D. Rodgers (1998), Retrieval of tropospheric carbon monoxide for the MOPITT experiment, *J. Geophys. Res.*, *103*, 32,277–32,290.
- Pierrehumbert, R. T. (2000), Lattice models of advection-diffusion, *Chaos*, *10*(1), 61–74, doi:10.1063/1.166476.
- Richard, A. C., et al. (2006), High-resolution airborne profiles of CH₄, O₃, and water vapor near tropical Central America in late January to early February 2004, *J. Geophys. Res.*, *111*, D13304, doi:10.1029/2005JD006513.
- Rodgers, C. D. (2000), *Inverse Methods for Atmospheric Sounding: Theory and Practice*, 238 pp., World Sci., Tokyo.
- Ryoo, J. M., T. Igusa, and D. W. Waugh (2009), PDFs of tropical tropospheric humidity: Measurements and theory, *J. Clim.*, *22*, 3357–3373.
- Schertzer, D., and S. Lovejoy (1985), The dimension and intermittency of atmospheric dynamics, in *Turbulent Shear Flows 4*, edited by B. Launder, pp. 7–33, Springer, New York.
- Shraiman, B. I., and E. D. Siggia (1994), Lagrangian path integrals and fluctuations in random flow, *Phys. Rev. E*, *49*, 2912–2927, doi:10.1103/PhysRevE.49.2912.
- Sparling, L. C., and J. T. Baumeister (2001), Scale dependence of tracer microstructure: PDFs, intermittency and the dissipation scale, *Geophys. Res. Lett.*, *28*, 2823–2826.
- Suntharalingam, P., C. M. Spivakovsky, J. A. Logan, and M. B. McElroy (2003), Estimating the distribution of terrestrial CO₂ sources and sinks from atmospheric measurements: Sensitivity to configuration of the observation network, *J. Geophys. Res.*, *108*(D15), 4452, doi:10.1029/2002JD002207.

Zhang, C., B. Mapes, and B. Soden (2003), Bimodality in tropical water vapor, *Q. J. R. Meteorol. Soc.*, 129, 2847–2866, doi:10.1256/qj.02.166.

Q. B. Li, B. R. Lintner, J. D. Neelin, S. N. Stechmann, and L. Zhang, Department of Atmospheric and Oceanic Sciences, University of California, Los Angeles, CA 90095-1565, USA. (neelin@atmos.ucla.edu)

P. K. Patra, Frontier Research Center for Global Change, 3173-25 Showa-machi, Kanazawa, Yokohama 236-0001, Japan.

M. T. Chahine and B. Tian, Jet Propulsion Laboratory, Pasadena, CA 91109, USA.